

Exosomal hsa_circ_0035277 enhances the malignancy of gastric cancer by interacting with the m⁶A reader ELAVL1

Ang Cai, Xiaokang Zhou

Department of Oncology, Wuhan Hospital of Traditional Chinese Medicine, Wuhan, Hubei, China

Submitted: 22 August 2023; **Accepted:** 2 January 2024

Online publication:

Arch Med Sci

DOI: <https://doi.org/10.5114/aoms/178185>

Copyright © 2024 Termedia & Banach

Corresponding author:

Xiaokang Zhou

Department of Oncology

Wuhan Hospital of

Traditional Chinese

Medicine

49 Lihuangpi Road

Jiangan District

Wuhan 430014

Hubei, China

Phone: +86 15527061589

E-mail:

zhouxiaokang123456@126.

com

Abstract

Introduction: Exosome-derived circular RNA (circRNA) and N⁶-methyladenosine (m⁶A) modifications have been found to play key regulatory functions in gastric carcinogenesis (GA). This study investigated the detailed mechanism of exosomal hsa_circ_0035277 in the development of GA.

Material and methods: The survival rate of GA patients was analyzed using log-rank (Mantel-Cox) tests. GA cell exosomes were extracted, exosomal marker proteins were detected using western blot, and hsa_circ_0035277 knockdown exosomes were co-cultured with gastric cancer cells. Quantitative real-time polymerase chain reaction was used to detect hsa_circ_0035277 and embryonic lethal-abnormal vision-like protein 1 (ELAVL1) levels in GA. Transwell, colony formation, Cell Counting Kit-8, and *in vivo* assays were used to evaluate GA cell malignancy. Subsequently, we performed methylated RNA immunoprecipitation (MeRIP) and RNA immunoprecipitation (RIP) assays to analyze the m⁶A modification effect of ELAVL1 on hsa_circ_0035277.

Results: We observed that hsa_circ_0035277 was abundantly expressed in GA, and its high expression levels could accurately predict the poor survival rate of GA patients. The proliferative and migratory capacity of GA cells could be inhibited by knocking down hsa_circ_0035277 or co-culturing with exosomes knocking down hsa_circ_0035277. *In vivo*, knocking down hsa_circ_0035277 also inhibited tumor growth. In addition, ELAVL1 was found to promote the stable expression of hsa_circ_0035277 by regulating its m⁶A level.

Conclusions: Exosomal hsa_circ_0035277 was m⁶A-modified by the m⁶A reader ELAVL1 to stabilize its expression, which in turn promoted malignancy in gastric cancer cells. These findings provide a potential target for clinical diagnosis and treatment of GA.

Key words: exosome, hsa_circ_0035277, gastric cancer, m⁶A reader, ELAVL1.

Introduction

In 2020, the global incidence rate of gastric cancer (GA) was 11.1 cases per 100,000, causing more than 750,000 deaths [1]. In the same year, there were more than 470,000 GA cases, leading to 370,000 deaths, in China, accounting for 43.94% and 48.62% of global GA cases and deaths, respectively [1]. Given that the majority of GA cases are

diagnosed at an intermediate to advanced stage of metastasis, current treatment options do not significantly improve the survival prognosis for GA patients [2]. Several studies have shown that multiple tumor-promoting or tumor-suppressing genes can regulate the progression of GA [3, 4], making it urgent to actively explore the mechanism of GA development and enhance the therapeutic effect and prognosis for GA patients

With the development of genome-wide molecular targeting, the diversity of molecular changes during tumor progression has been revealed [5]. Circular RNAs (circRNAs) are produced from precursor mRNAs that link the 5'UTR end of linear mRNAs to the 3'UTR end by a "reverse splicing" mechanism. Numerous studies have shown that the unique epitopes of circRNAs exert multifaceted regulatory functions in numerous diseases, including malignant tumor progression [6–10]. For example, high expression of circNFATC3 in GA is positively correlated with tumor volume, and its knockdown decreases the proliferation of GA cells [11]. Furthermore, exogenous circ_0003356 has been found to inhibit migration, viability, proliferation, epithelial-mesenchymal transition, and invasion, and enhance apoptosis in GA cells [12]. According to the data obtained from the circBase database (<http://www.circbase.org>), hsa_circ_0035277, with a length of 223 nt, is located at chr15:51743841-51747425, and it is encoded from the linear transcript DMXL2. A rare circRNA microarray assessment in GA patients and healthy controls highlighted the presence of elevated hsa_circ_0035277 levels in the plasma of GA patients [13]. Therefore, this study aimed to investigate the effect and mechanism of hsa_circ_0035277 in the development of GA.

Exosomes, extracellular vesicles released from eukaryotic cells, have been associated with a variety of disease processes [14]. In cancer, tumor-derived exosomes have been found to regulate cancer cell migration, invasion, as well as pre-metastasis through paracrine subversion of local and distant microenvironments [15]. Zhang *et al.* [16] observed that circNRIP1, which is up-regulated in GA, could promote tumor metastasis *in vivo* through exosomal dissemination among GA cells. Furthermore, Yang *et al.* [17] found that circ_0063526, whose expression levels are elevated in cisplatin-resistant GA, was assimilated into exosomes and delivered to cisplatin-sensitive GA cells, thereby enhancing cisplatin resistance. In addition, the authors confirmed that silencing of exosome circ_0063526 could suppress cisplatin resistance by inhibiting migration, invasion, and autophagy in GA cells. However, it is not yet known whether exosomal hsa_circ_0035277 is involved in GA progression.

N6-Methyladenosine (m⁶A), a class of post-transcriptional modifications most abundant in mammalian mRNAs, plays a crucial role in mRNA stability, decay, nuclear retention, and translational control regulation [18]. Previous studies have shown that m⁶A participates in the degradation of mRNAs by modifying their 5'UTR, while at the same time contributing to mRNA nucleation, translation, and maintenance of structural stability via 3'UTR modifications [19, 20]. As a dynamic regulatory system, the overall m⁶A modification level is adjusted through its methyltransferases, demethylases, and read proteins [21], and the involvement of m⁶A in GA regulation has been reported. For example, the methyltransferase METTL14 inhibits circORC5 expression by targeting m⁶A modification, which in turn suppresses GA cell metastasis [22]. Hsa_circRNA_0077837 expression in GA has been found to correlate with m⁶A modification, and the lower the degree of its expression, the higher are the m⁶A levels [23]. Nevertheless, the effect of m⁶A modification of hsa_circ_0035277 in GA remains unknown.

This study focused on the differential level of hsa_circ_0035277 in GA and its effect on the malignant behavior of GA cells. In addition, we explored the molecular mechanisms by which m⁶A modification of exosome hsa_circ_0035277 affects GA progression. The present study provides novel evidence that GA-derived exosomal circRNA can potentially be used as a biomarker for GA diagnosis.

Material and methods

Tissue samples

Thirty-four pairs of GA tissues, as well as adjacent noncancerous tissues, were obtained from surgically resected patients admitted to the Wuhan Hospital of Traditional Chinese Medicine, and tissues with GA were confirmed by at least two pathologists. The present study was approved by the Ethics Committee of Wuhan Hospital of Traditional Chinese Medicine, and written informed consent was obtained from all participants. All clinicopathological features of patients are summarized in Table I.

Cell culture

We purchased GES-1, NCI-N87, HGC-27, and AGS cell lines from Procell (China). HGC-27, NCI-N87, and GES-1 cells were cultured in a basal RPMI-1640 medium (Procell), while AGS cells were cultured in Ham's F-12 medium (Procell). All culture media contained 1% P/S (Procell) and 10% fetal bovine serum (FBS, Procell), and all cells were maintained at 37°C with 5% CO₂.

Cell transfection

The ELAVL1 overexpression vectors (ELAVL1-OE) were constructed using pcDNA 3.1, with empty vectors (OE-NC) as the control. Two shRNAs for hsa_circ_0035277 (75 nM, sh-circ-1, sh-circ-2) were utilized to silence hsa_circ_0035277, and a shRNA non-targeting control (75 nM, shNC) was used as the control. All vectors were purchased from RiboBio (China) and delivered into AGS as well as HGC-27 cells by Lipo6000 (Beyotime, China). After 48 h, the transfection efficiency was measured through quantitative real-time polymerase chain reaction (qRT-PCR).

qRT-PCR assay and RNase R treatment

We used a total RNA Extraction Kit (Genexay Biotech, China) to harvest RNA. Additionally, a HiScript 1st Strand cDNA Synthesis Kit (Vazyme, China) was employed for cDNA generation. To quantify the amount of hsa_circ_0035277 and ELAVL1, we used the SYBR qPCR Master Mix (Vazyme) with GAPDH standardization and the $2^{-\Delta\Delta Ct}$ method. All primers are summarized in Table II.

In addition, cell RNA was incubated with RNase R (Zeye Biotech, China) at 37°C for 30 min to ensure that RNA enzyme digestion would remove all linear RNA. Then, the collected RNA was amplified to generate cDNA, hsa_circ_0035277, and its linear transcript (DMXL2) was measured to evaluate hsa_circ_0035277 stability.

Exosome extraction, identification, and co-culture

AGS cells transfected with shNC and sh-circ-2 were cultured for 48 h, and the medium was then collected and used to extract the exosomes. The medium was sequentially centrifuged at 1000 × g for 10 min, 3000 × g for 30 min, and 10000 × g for 60 min at 4°C. After the centrifugation step, the supernatant was extracted and filtered through a polyvinylidene difluoride (PVDF) membrane (0.22 μm) to sequentially remove dead cells, cell debris, and displaced vesicles. Finally, the supernatant was centrifuged at 100 000 × g for 4 h, and the exosome precipitate was then harvested. Expression of CD63 and CD81, which are characteristic proteins on the exosomes surface, were measured by western blot assay. For co-culture, 30 μg of exosomes were placed in a 12-well plate and 1 × 10⁶ HGC-27 or AGS

Table I. Clinical characteristics of the gastric cancer patients (n = 34)

Variables	N	%
Age		
< 60	12	35.5
≥ 60	22	64.7
Sex		
Male	25	73.5
Female	9	26.5
Tumor size (diameter) [cm]		
< 5	18	52.9
≥ 5	16	47.1
Differentiation		
Well	5	14.7
Moderate	16	47.1
Poor	13	38.2
Lymphatic metastasis		
Absent	8	23.5
Present	26	76.5
Peritoneal metastasis		
Absent	25	73.5
Present	9	26.5
TNM stage		
I-II	16	47.1
III-IV	18	52.9

cells, respectively, were added. After 48 h of incubation, the cells were analyzed to assess their biological functions.

Western blot assay

Proteins were extracted using RIPA Lysis Buffer (Beyotime, China), and were subsequently determined via the Enhanced BCA Protein Assay Kit (Beyotime) after electrophoresis in a sodium dodecyl sulfate-polyacrylamide gel (10%). Subsequently, proteins were delivered onto the PVDF membranes and blocked with 5% bovine serum albumin at 25°C for 2 h. Thereafter, the primary antibodies, namely anti-CD63 (abs159125, Absin, China), anti-CD81 (abs159270, Absin), anti-ELAVL1 (abs115647, Absin), and anti-GAPDH (abs132004, Absin), were incubated with membranes at 4°C overnight. After washing, the membrane was incubated with secondary anti-Rabbit IgG antibody (A0208, Beyotime) for 1 h at 37°C.

Table II. Primer sequences used in this study

Gene	Forward primer (5'-3')	Reverse primer (5'-3')
hsa_circ_0035277	AATGTTTGCCTCTGGGACAC	TGTGGCTTTACTGTGGCACT
DMXL2	GCTTTGGCTGATACAGTGGCTAC	GGCAGCGATGTCAAAGGCATG
GAPDH	GAGAAGGCTGGGCTCATT	AGTGATGGCATGGACTGTGG

BeyoECL Plus (P0018S, Beyotime) was applied for band visualization, and ImageJ software for used to evaluate the protein levels.

Cell counting Kit-8 (CCK-8) assay

The treated cells (1×10^4 /ml) were cultured in a 96-well plate for 0, 24, 48, and 72 h. Subsequently, the optical density (OD) values were evaluated under a microplate reader (Molecular Devices, China) at 450 nm after cultivation with a CCK-8 solution (10 μ l/well, Beyotime, China) for another 4 h.

Colony formation assay

AGS as well as HGC-27 cells (2×10^3 /ml) were transferred to the corresponding 6-well plates at 1 ml per well. After 14 days of cell culture, the supernatant was removed and washed. Paraformaldehyde (4%) was added and fixed at 25°C for 10 min, and a crystalline violet staining solution (700 μ l) was added and stained for 5 min. The plates were dried and photographed using a light microscope (Olympus, Japan).

Transwell migration assay

Firstly, a serum-free medium (200 μ l) containing 1×10^4 AGS and HGC-27 cells was added to the upper chamber of a Transwell, while a medium with 10% FBS (600 μ l) was added to the bottom chamber. After 24 h, migrated cells were fixed with paraformaldehyde and stained with crystal violet. The cell migratory ability was evaluated using a microscope (Olympus).

In vivo experiment

A total of 12 male nude mice (4–6 weeks, $n = 3$ /group) were purchased from Shulaibao Biotechnology Co., Ltd. (China). 1×10^6 AGS cells transfected with shNC, sh-circ-2, NC-OE, or ELAVL1-OE were subcutaneously injected into the nude mice. The tumor volume was assessed every week using a digital caliper to measure tumor width and length. After 4 weeks, the mice were euthanized, and the tumor was removed to confirm its weight.

Immunohistochemistry (IHC) assay

The tissue sections from nude mice were treated with 3% hydrogen peroxide after deparaffinizing and dehydrating. Then, anti-Ki67 (abs145260, Absin, China) or anti-ELAVL1 (abs115647, Absin) was used to incubate slices at 4°C overnight. After incubation with secondary antibody for 1 h, the sections were treated with 3'-diaminobenzidine tetrahydrochloride and counterstained with hematoxylin.

RNA m⁶A quantification assay

An EpiQuik m6A Kit (A-P-9005, A&D Technology, China) was utilized to measure the m⁶A modification level of total RNA in GES-1, AGS, and HGC-27 cells. Briefly, m⁶A standards and RNA (200 ng) were added to the assay wells and mixed to detect m⁶A using capture and detection antibodies. Finally, m6A levels were quantified by recording their OD at 450 nm (OD450).

Methylated RNA immunoprecipitation (MeRIP)-qPCR

We employed the Magna MeRIP m6A kit (Millipore, USA) to conduct this experiment. Briefly, 1×10^7 AGS and HGC-27 cells were lysed with lysis buffer. After removal of DNA, 20 μ l of protein A/G beads conjugated with anti-IgG or anti-m⁶A antibody were added and incubated overnight at 4°C. After extraction of RNA, the hsa_circ_0035277 m⁶A-methylated level was detected via qRT-PCR.

RNA immunoprecipitation (RIP) assay

We used the RIP assay kit (R&S Biotechnology, China) to analyze the interaction between hsa_circ_0035277 and ELAVL1. The magnetic beads were pretreated with anti-ELAVL1 (ab200342, Abcam, UK) or IgG antibody for 30 min at 25°C. Meanwhile, AGS as well as HGC-27 cells were lysed via RNA lysis buffer. The incubated magnetic beads were mixed with the cell lysate at 4°C overnight. After washing, the hsa_circ_0035277 level was measured by qRT-PCR.

RNA stabilization assay

Actinomycin D (2 μ g/ml, transcriptional inhibitor) was incubated with AGS as well as HGC-27 cells treated with ELAVL1-OE or NC-OE for 0, 8, 16, and 24 h to block transcription. Subsequently, cells were collected for RNA extraction, and hsa_circ_0035277 levels were measured via qRT-PCR.

Statistical analysis

Data are presented as mean \pm SD using GraphPad Prism software (v. 8.0, GraphPad, USA). A *p*-value of < 0.05 was considered statistically significant. Differences between the two groups were evaluated using Student's *t*-test, and those among multiple groups were assessed by one-way ANOVA. Log-rank (Mantel-Cox) tests were applied to evaluate the correlation between the hsa_circ_0035277 expression group and the survival rate of GA patients. Fisher's exact test was used to analyze the correlation between hsa_circ_0035277 expression and clinical characteristics.

Results

hsa_circ_0035277 is highly expressed in GA

Firstly, we analyzed the microarray dataset of GEO, GSE93541, which showed that hsa_circ_0035277 was highly expressed in GA

samples (Figure 1 A). Secondly, our findings revealed that hsa_circ_0035277 had a ring-like structure (Figure 1 B). We then used RNase processing to identify any insignificant changes in hsa_circ_0035277 expression between the RNase R group and the mock group. DMXL2 (lin-

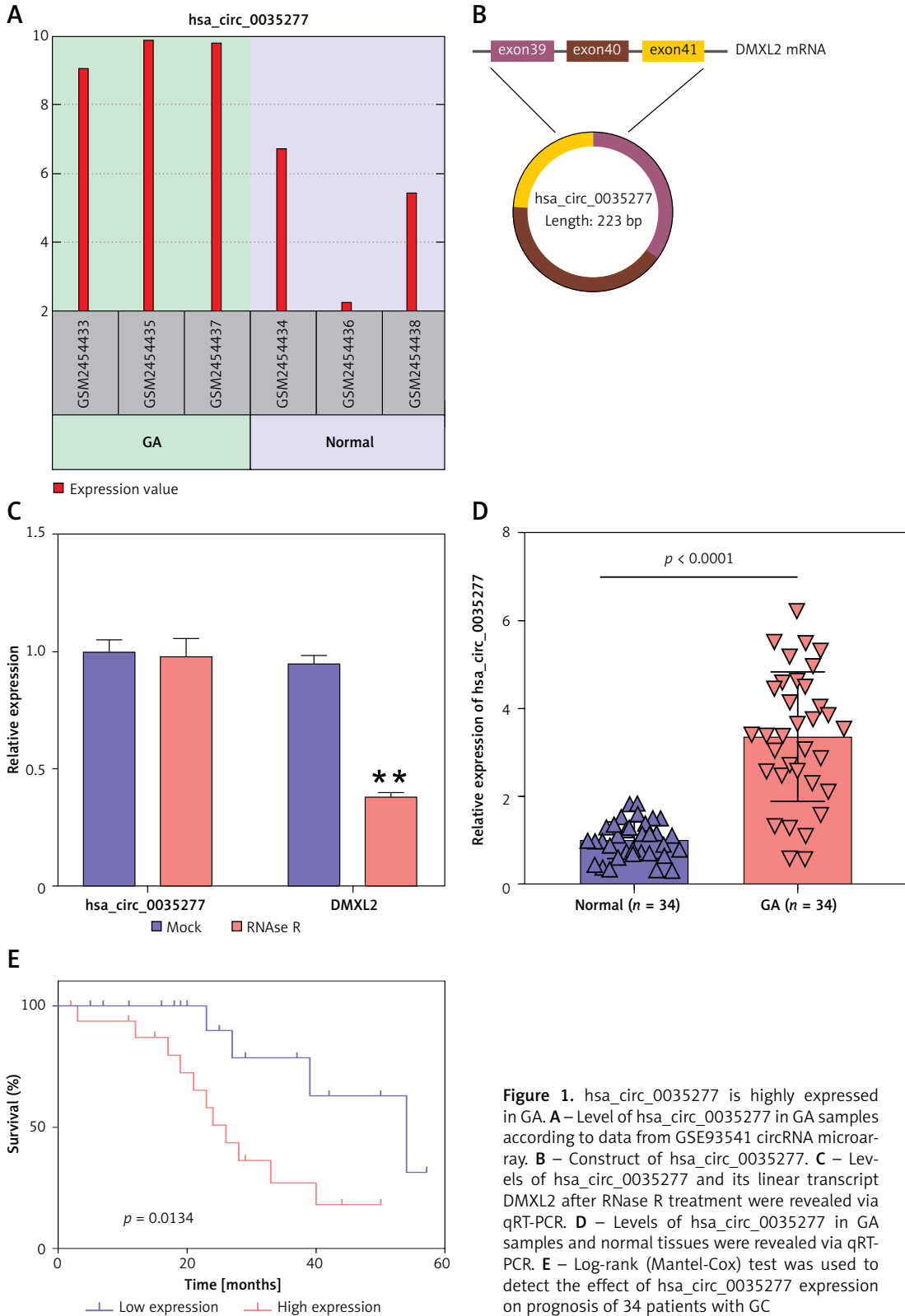


Figure 1. hsa_circ_0035277 is highly expressed in GA. **A** – Level of hsa_circ_0035277 in GA samples according to data from GSE93541 circRNA microarray. **B** – Construct of hsa_circ_0035277. **C** – Levels of hsa_circ_0035277 and its linear transcript DMXL2 after RNase R treatment were revealed via qRT-PCR. **D** – Levels of hsa_circ_0035277 in GA samples and normal tissues were revealed via qRT-PCR. **E** – Log-rank (Mantel-Cox) test was used to detect the effect of hsa_circ_0035277 expression on prognosis of 34 patients with GC

ear transcript of hsa_circ_0035277) was found to be significantly reduced, confirming the circular structure of hsa_circ_0035277 (Figure 1 C). Additionally, the 34 pairs of tissues were analyzed via qRT-PCR analysis, and the data showed that the hsa_circ_0035277 levels in GA tissues were least 3.5 times higher than in normal tissues (Figure 1 D). Log-rank (Mantel-Cox) tests demonstrated that the hsa_circ_0035277 high-expression group's survival rate decreased with increasing time (Figure 1 E). Moreover, high expression of hsa_circ_0035277 was correlated with a greater tumor size, peritoneal metastasis, and higher tumor node metastasis (TNM) stage (Table III). These findings suggest that the presence of hsa_circ_0035277 with a circular structure, which was highly expressed in GA samples, could predict poor patient prognosis.

Silencing of hsa_circ_0035277 inhibits GA malignancy

qRT-PCR revealed that hsa_circ_0035277 was 1.5-, 3.5-, and 4.5-fold higher in NCI-N87, AGS, and HGC-27 cells, respectively, than in GES-1 cells (Figure 2 A). AGS as well as HGC-27 cells with high hsa_circ_0035277 levels were used for our subsequent studies. CCK-8 results indicated that

cell viability was downregulated in AGS and HGC-27 cells following hsa_circ_0035277 knockdown (Figure 2 B). In addition, compared to the shNC group, the ability of plate colony formation was inhibited in both sh-circ-1 and sh-circ-2 groups (Figure 2 C). Moreover, Transwell data revealed that AGS and HGC-27 cell migration was lower in both sh-circ-1 and sh-circ-2 groups compared with the shNC group (Figure 2 D). Owing to the increased inhibitory effect of sh-circ-2 on GA cells, we used AGS transfected with sh-circ-2 to inject nude mice for our *in vivo* experiment, which further confirmed that sh-circ-2 induced a smaller tumor size and volume, as well as lighter tumor weight (Figure 2 E). Detection of the proliferation marker Ki67 using IHC assay showed that the positive rate of Ki67 in the sh-circ-2 group was reduced by 50% (Figure 2 F). Thus, low expression of hsa_circ_0035277 restrains GA malignancy both *in vivo* and *in vitro*.

Exosome knockdown of hsa_circ_0035277 inhibits GA malignancy

Supernatants from AGS cells, either untransfected or transfected with shNC or sh-circ-2 (renamed sh-circ), were collected, treated with centrifugation, and the marker proteins of exo-

Table III. Correlations between hsa_circ_0035277 expression and clinical characteristics

Variables	hsa_circ_0035277 expression		P-value
	Low (n = 15)	High (n = 19)	
Age			> 0.9999
< 60	5	7	
≥ 60	10	12	
Sex			0.4620
Male	10	15	
Female	5	4	
Tumor size (diameter) [cm]			0.0070
< 5	12	6	
≥ 5	3	13	
Differentiation			0.1495
Well	3	2	
Moderate	9	7	
Poor	3	10	
Lymphatic metastasis			0.2569
Absent	2	6	
Present	13	13	
Peritoneal metastasis			0.0042
Absent	7	18	
Present	8	1	
TNM stage			< 0.0001
I-II	13	3	
III-IV	2	16	

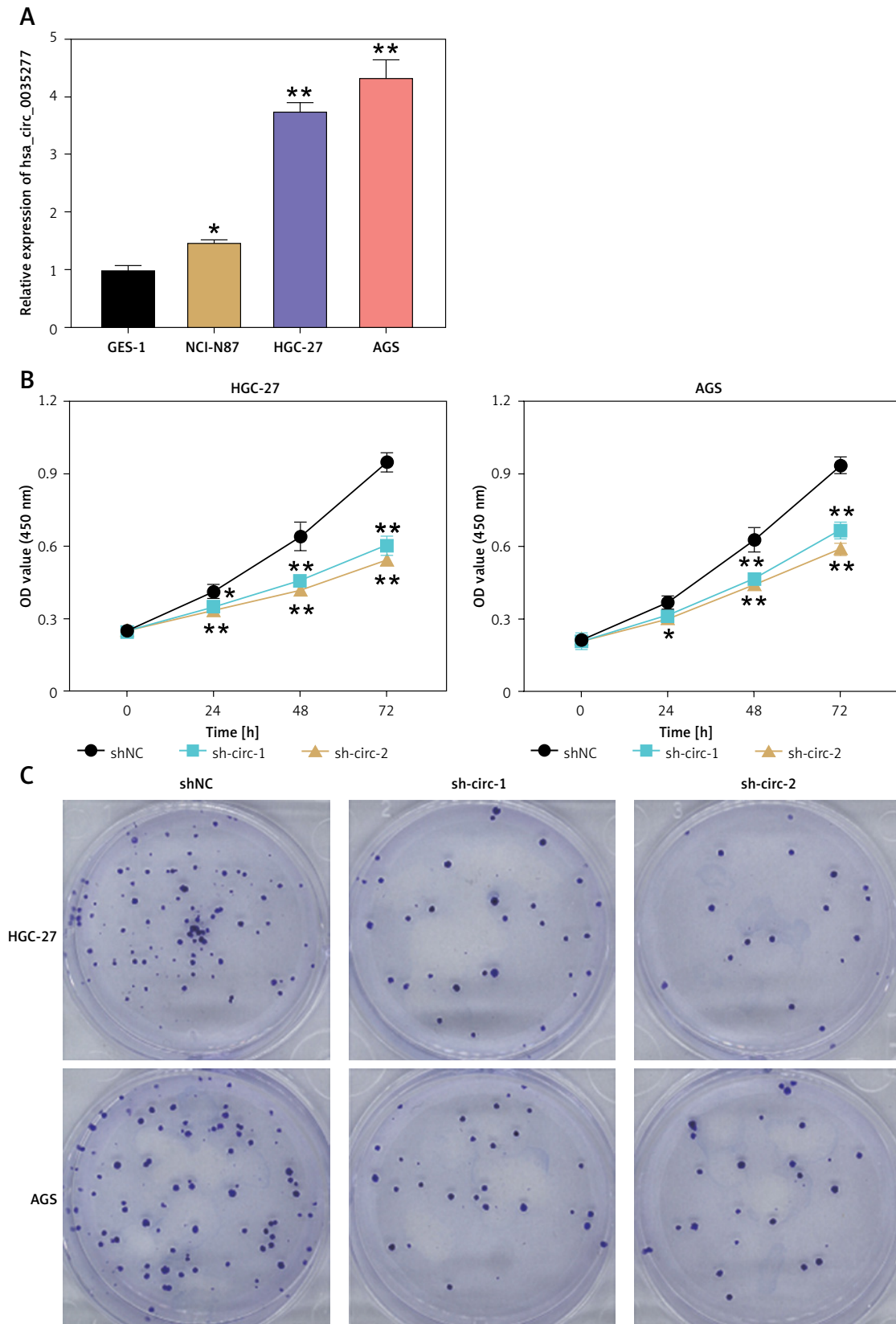
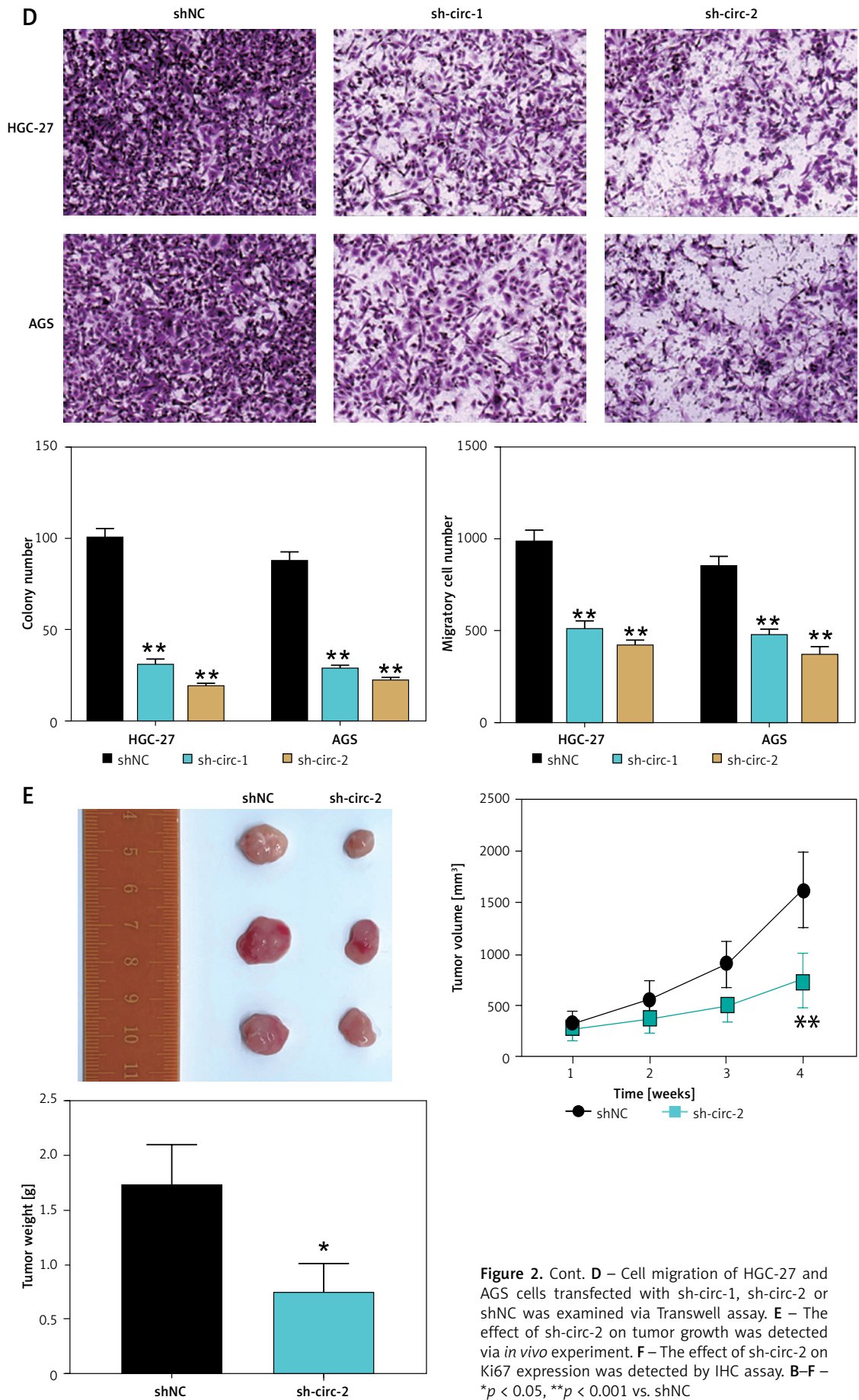


Figure 2. Silencing of hsa_circ_0035277 inhibits GA malignancy. **A** – Levels of hsa_circ_0035277 in GES-1, NCI-N87, HGC-27, and AGS cell lines were determined via qRT-PCR. * $P < 0.05$, ** $P < 0.001$ vs. GES-1. **B** – Cell viability of HGC-27 and AGS cells transfected with sh-circ-1, sh-circ-2 or shNC was assessed via CCK-8 assay. **C** – Cell proliferation of HGC-27 and AGS cells transfected with sh-circ-1, sh-circ-2 or shNC was revealed via colony formation assay. **B-F** – * $p < 0.05$, ** $p < 0.001$ vs. shNC



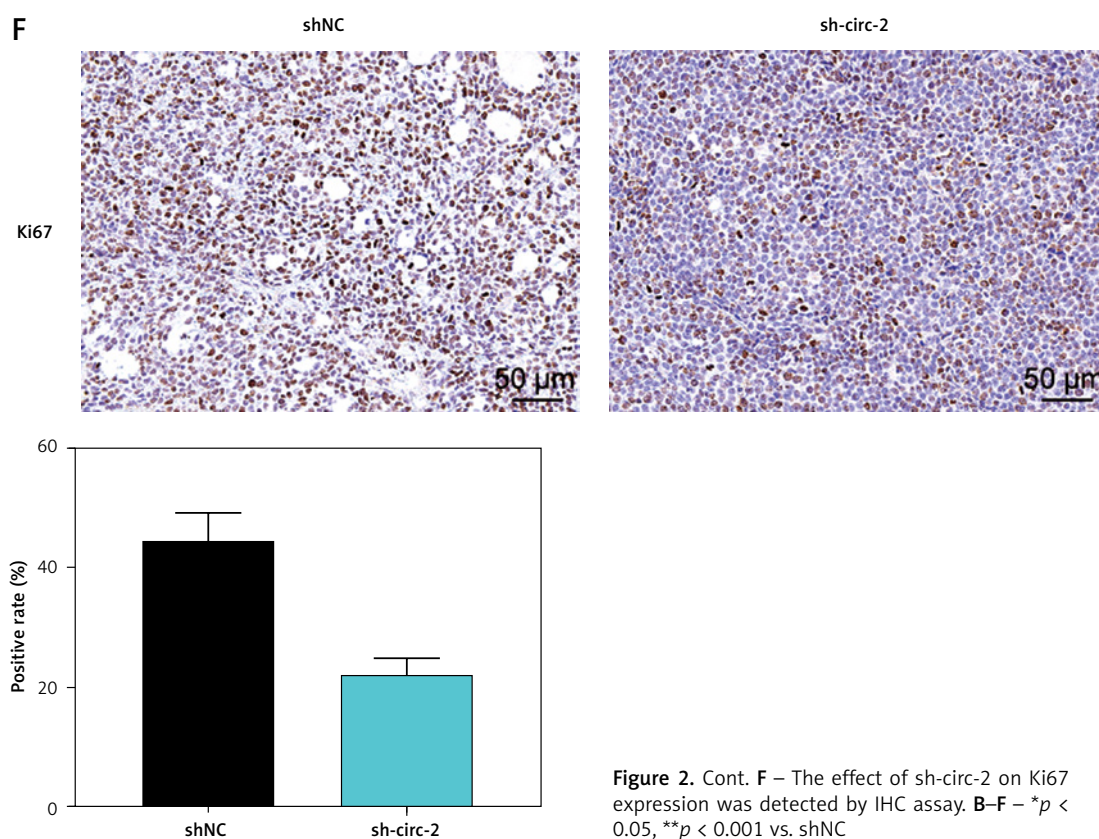


Figure 2. Cont. **F** – The effect of sh-circ-2 on Ki67 expression was detected by IHC assay. **B–F** – * $p < 0.05$, ** $p < 0.001$ vs. shNC

somes were then detected. The lower CD63 and CD81 protein levels in cell extracts compared to exosomes revealed that GA cell exosomes were successfully collected (Figure 3 A). Subsequently, the exosomes of AGS cells that were not transfected, transfected with shNC or transfected with sh-circ were co-cultured with AGS and HGC-27 cells to obtain the Control, Exo-shNC, and Exo-sh-circ groups, respectively. Our findings showed that cell proliferation levels in the Exo-sh-circ group were downregulated compared to the Control and Exo-shNC groups (Figures 3 B, C), whereas cell migration levels in Exo-sh-circ were lower than those in the Control and Exo-shNC groups (Figure 3 D). Our results clearly suggest that exosomes of GA cells with silenced hsa_circ_0035277 expression could effectively suppress the malignant phenotype of other strains of GA cells.

ELAVL1 regulates the m⁶A modification of hsa_circ_0035277

Next, we elucidated the regulatory mechanism of hsa_circ_0035277 in GA cells. Quantification of RNA m⁶A showed that the m⁶A levels were upregulated in both AGS and HGC-27 cells compared to GES-1 (Figure 4 A). Moreover, MeRIP exhibited increased m⁶A levels of hsa_circ_0035277 in both AGS and HGC-27 cells (Figure 4 B), while RBPDB predicted the interaction between ELAVL1 and

hsa_circ_0035277 (Figure 4 C). After transfecting ELAVL1 overexpression vectors into GA cells, the protein levels of ELAVL1 were enhanced (Figure 4 D). Then, the MeRIP assay demonstrated an increase in the m⁶A levels of hsa_circ_0035277 in GA cells after ELAVL1 overexpression (Figure 4 E). Further analysis showed that ELAVL1 antibody enriched hsa_circ_0035277 levels in GA cells (Figure 4 F), while the RNA stabilization assay further showed that ELAVL1 upregulation could stabilize hsa_circ_0035277 levels (Figure 4 G). Finally, it was revealed that ELAVL1 increased the m⁶A levels of hsa_circ_0035277 by binding to hsa_circ_0035277, thereby increasing hsa_circ_0035277 expression.

ELAVL1 overexpression enhances GA malignancy *in vitro*

The effects of ELAVL1 on GA malignancy were confirmed by both *in vitro* and *in vivo* experiments. First, the CCK-8 assay showed that ELAVL1 overexpression enhanced cell viability in both AGS and HGC-27 cells (Figure 5 A). The ability to form colonies was also enhanced by ELAVL1 overexpression in GA cells (Figure 5 B). Second, the Transwell assay revealed that ELAVL1 overexpression induced an increase in AGS and HGC-27 cell migration (Figure 5 C). Overall, our findings confirmed the promotive effect of ELAVL1 overexpression on GA malignancy *in vitro*.

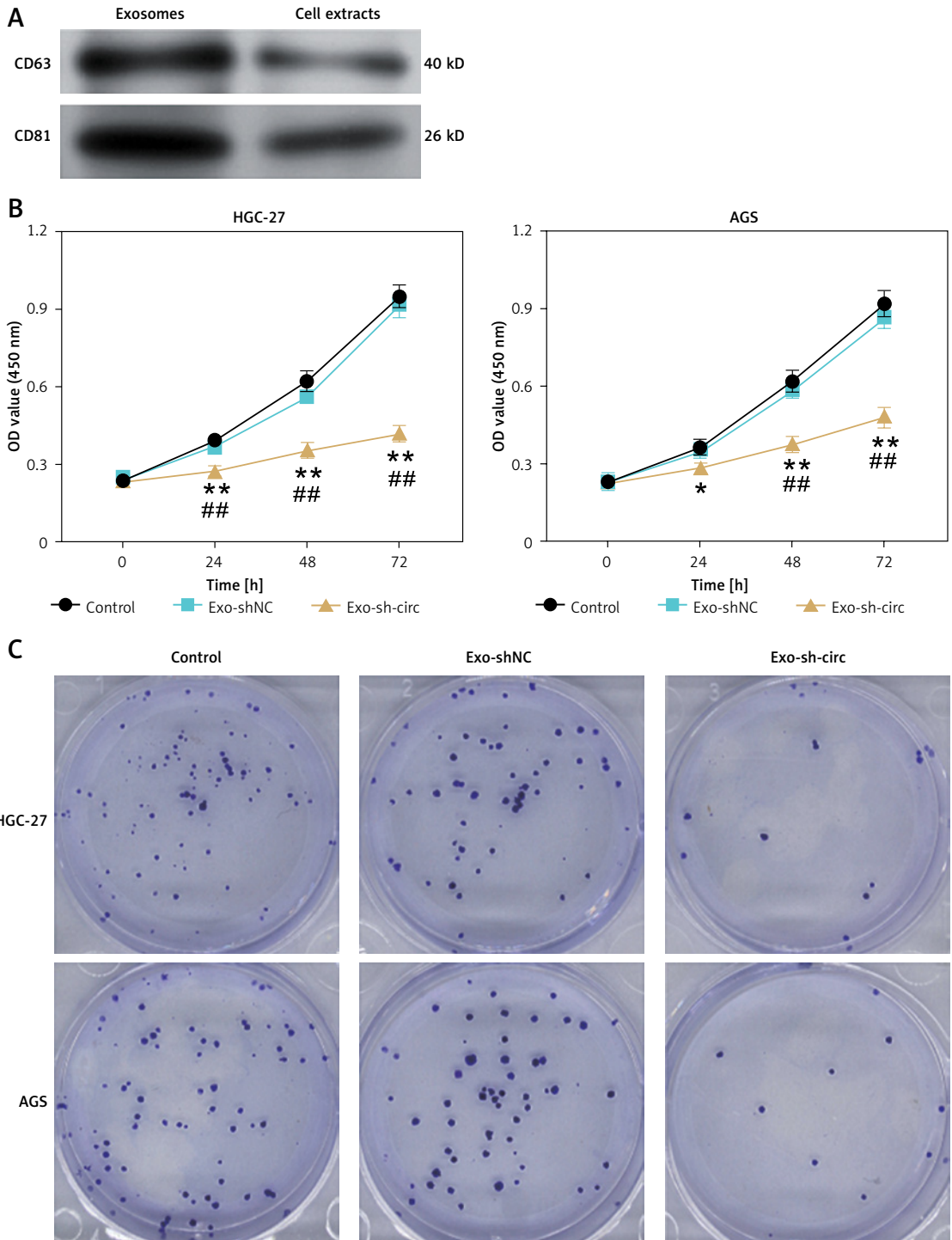


Figure 3. Exosome knockdown of hsa_circ_0035277 inhibits GA malignancy. **A** – The exosome markers (CD63 and CD81) were detected by western blot analysis. **B** – Cell viability of HGC-27 and AGS cells in Control, Exo-shNC, and Exo-sh-circ groups was revealed via CCK-8 assay. **C** – Cell proliferation of HGC-27 and AGS cells in Control, Exo-shNC, and Exo-sh-circ groups was revealed via colony formation assay. **B–D** – Control group; exosomes from non-transfected AGS were co-cultured with HGC-27 and AGS cells. **p* < 0.05, ***p* < 0.001 vs. Control; ##*p* < 0.001 vs. Exo-shNC

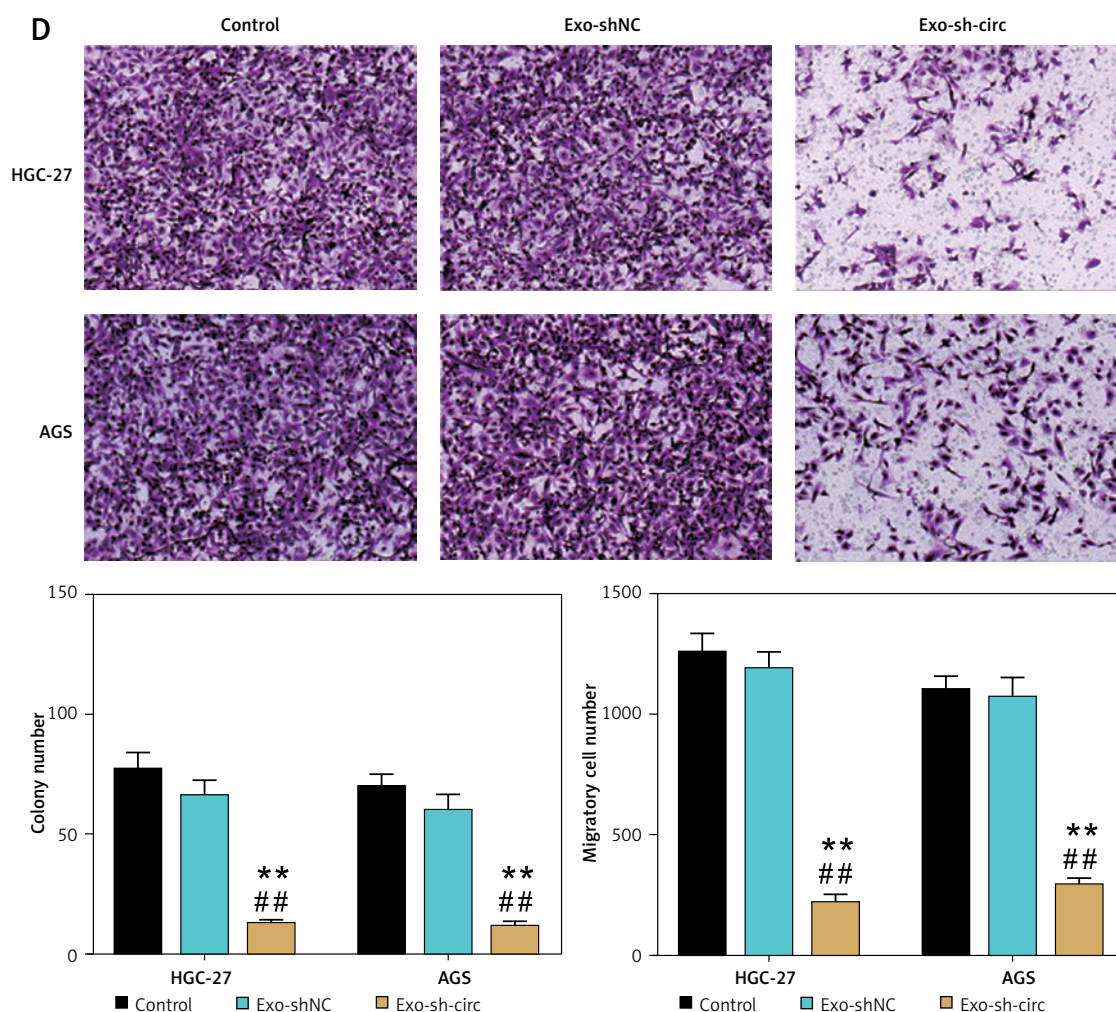


Figure 3. Cont. **D** – Cell migration of HGC-27 and AGS cells in Control, Exo-shNC, and Exo-sh-circ groups was revealed via Transwell assay. **B–D** – Control group; exosomes from non-transfected AGS were co-cultured with HGC-27 and AGS cells. * $p < 0.05$, ** $p < 0.001$ vs. Control; ## $p < 0.001$ vs. Exo-shNC

ELAVL1 overexpression promotes tumor growth *in vivo*

An *in vivo* experiment further confirmed the role of ELAVL1 overexpression on tumor growth. As shown in Figure 6 A, ELAVL1 overexpression was associated with greater tumor size, volume, and weight. IHC assay proved that the positive rate of Ki67 was increased when the positive rate of ELAVL1 increased (Figure 6 B). These data indicated the positive effect of ELAVL1 overexpression on tumor growth *in vivo*.

Discussion

The present study confirmed the high expression levels of hsa_circ_0035277 in GA and also its silencing effect on attenuating the tumorigenic behavior of cancer cells. In addition, we found that GA cell-derived exosomes could deliver knockdown hsa_circ_0035277 to the target GA cells and inhibit target GA cell malignancy. No-

tably, our results showed that hsa_circ_0035277 was m⁶A-modified by ELAVL1 to promote its stable expression. This in turn provides novel ideas for screening but also inhibiting GA progression.

Exosomes are surrounded by a lipid bilayer secreted by most cells, and were initially recorded as waste products produced by cells, which had no effect on their neighboring cells [24]. Recently, research studies have shown that exosomes reprogram target cells by transporting complex components, such as nucleic acids, lipids, and proteins, that they already carry [25]. Current research suggests that cancer progression occurs as a consequence of a continuous exchange of information between tumor cells and their stromal microenvironment [26, 27]. Exosomes induce and promote a microenvironment conducive to tumorigenesis, thereby promoting tumor progression and survival [15]. In addition, the involvement of exosome-transported circRNA in cancer progression has long been reported. Yang *et al.* [28] found that

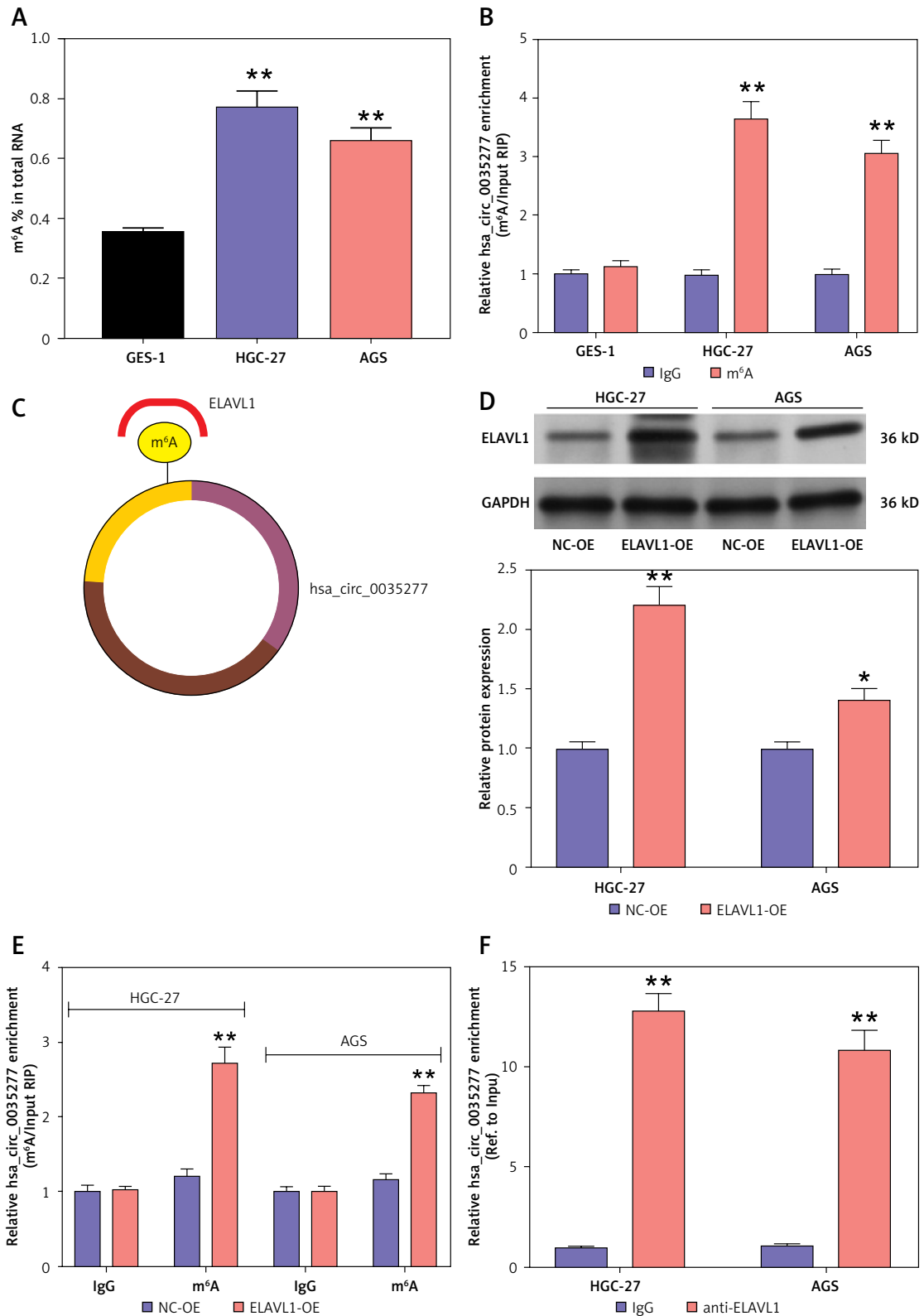


Figure 4. ELAVL1 regulates the m⁶A modification of hsa_circ_0035277. **A** – The content of m⁶A in GES-1, HGC-27, and AGS cell lines was revealed by RNA m⁶A quantification assay. ***P* < 0.001 vs. GES-1. **B** – The level of m⁶A modification of hsa_circ_0035277 was measured by MeRIP assay in GES-1, HGC-27, and AGS cell lines. ***P* < 0.001 vs. IgG. **C** – ELAVL1 was predicted to interact with hsa_circ_0035277 by RBPDB. **D** – Protein levels of ELAVL1 were detected by western blotting. **P* < 0.05, ***p* < 0.001 vs. NC-OE. **E** – The level of m⁶A modification of hsa_circ_0035277 was measured by MeRIP assay in HGC-27 and AGS cells transfected with NC-OE or ELAVL1-OE. ***P* < 0.001 vs. NC-OE. **F** – Enrichment level of hsa_circ_0035277 conjugated with IgG or anti-ELAVL1 in HGC-27 and AGS cells by RIP assay. ***P* < 0.001 vs. IgG

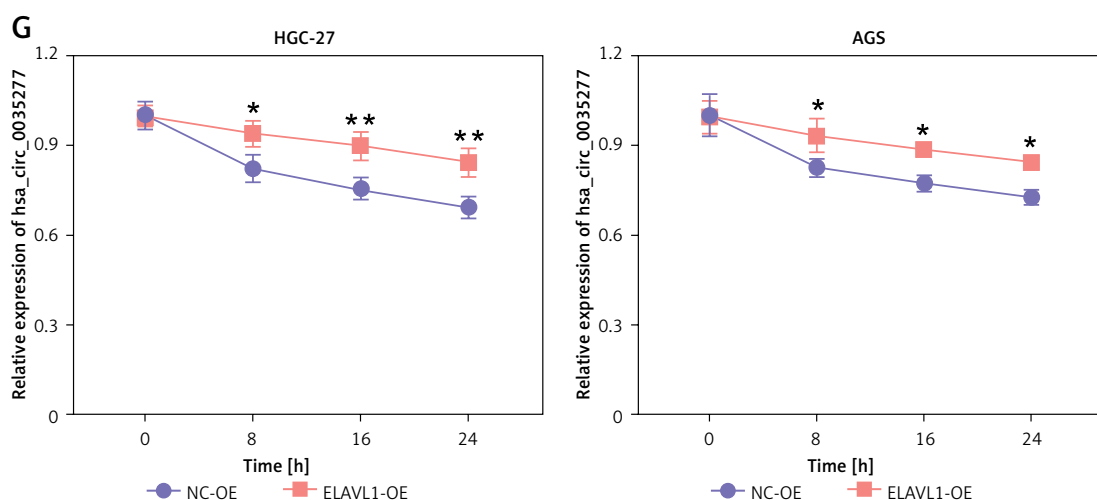


Figure 4. Cont. **G** – The levels of hsa_circ_0035277 in HGC-27 and AGS cells transfected with NC-OE or ELAVL1-OE after treatment with 2 µg/ml actinomycin D at the indicated time points were detected by qRT-PCR. * $P < 0.05$, ** $P < 0.001$ vs. NC-OE

silencing of exosome-derived hsa_circ_0085361 could inhibit bladder cancer cell metastasis and proliferation, and also suppress T-cell exhaustion. Furthermore, Zheng *et al.* [29] revealed that exosome circLPAR1 was significantly reduced during colorectal cancer development, although its levels recovered after surgery, and that its internalization by cancer cells could inhibit tumor growth. Xie *et al.* [30] reported that circSHKBP1 was upregulated in GA serum and tissues, which was associated with advanced TNM and low survival rates, and that exosomes, which are upregulated by circSHKBP1, could promote angiogenesis, migration, and proliferation of GA cells. Here, we revealed for the first time that hsa_circ_0035277, which is upregulated in GA, inhibited the proliferation, migration, and tumor growth of GA cells upon knockdown. Furthermore, our results showed that knockdown of hsa_circ_0035277 could be delivered to the target GA cells via exosomes, which in turn inhibited the migration and proliferation of target GA cells. The exosome hsa_circ_0035277 was found to be a pro-cancer factor in GA.

Embryonic lethal-abnormal vision-like protein 1 (ELAVL1) is an important cancer-related RNA binding protein, whose expression in various tumors, including prostate [31], colorectal [32], and breast cancer, has been found to significantly promote tumor development. In recent years, ELAVL1 has been identified as a reader that binds to m⁶A sites of RNAs and increases RNA stability [31]. It has been shown that ELAVL1 mediates ZMYM1 m⁶A modification and subsequently promotes epithelial-mesenchymal transition in GA [33]. The present study showed that ELAVL1 was involved in m⁶A modification in GA, a result which is consistent with the findings of previous studies. In addition, ELAVL1 has been reported to bind to a variety

of circRNAs. For example, ELAVL1 is recruited by hsa_circ_0000848 to stabilize SMAD7 expression, which in turn regulates cardiomyocyte apoptosis [34]. CircDLC1 could bind to ELAVL1, reducing the correlation between ELAVL1 and MMP1 mRNA, suppressing MMP1 levels, and inhibiting liver cancer progression [35]. ELAVL1 physically binds to circAGO2 to promote GA metastasis *in vivo* [36]. To the best of our knowledge, our study is the first to demonstrate that ELAVL1 regulates m⁶A modification of hsa_circ_0035277 by binding to hsa_circ_0035277 in GA, which in turn stabilizes hsa_circ_0035277 levels. Therefore, the promotional effect of hsa_circ_0035277 on GA development can be achieved by mediating m⁶A modification via ELAVL1.

Although this study confirmed the function and mechanism of hsa_circ_0035277 in GA development, there are still several limitations. First, the regulatory effect of hsa_circ_0035277 in GA development is complex. It is reported that circRNAs can act as competing endogenous RNAs (ceRNA) to participate in GA progression by interacting with miRNAs [37–39]. However, whether hsa_circ_0035277 in GA can act as a ceRNA to regulate a key miRNA has not been reported. Therefore, it is essential to investigate whether a key miRNA in GA can interact with hsa_circ_0035277 in GA. Next, the key signaling pathway that can be regulated by hsa_circ_0035277 should be further confirmed in the future. In addition, ELAVL1 as an m⁶A reader may be regulated by m⁶A methyltransferases or demethylases in GA, which deserves further investigation.

In conclusion, this study for the first time revealed that hsa_circ_0035277 is upregulated in GA, and exosome-derived hsa_circ_0035277 is a pro-cancer factor in GA development. The in-

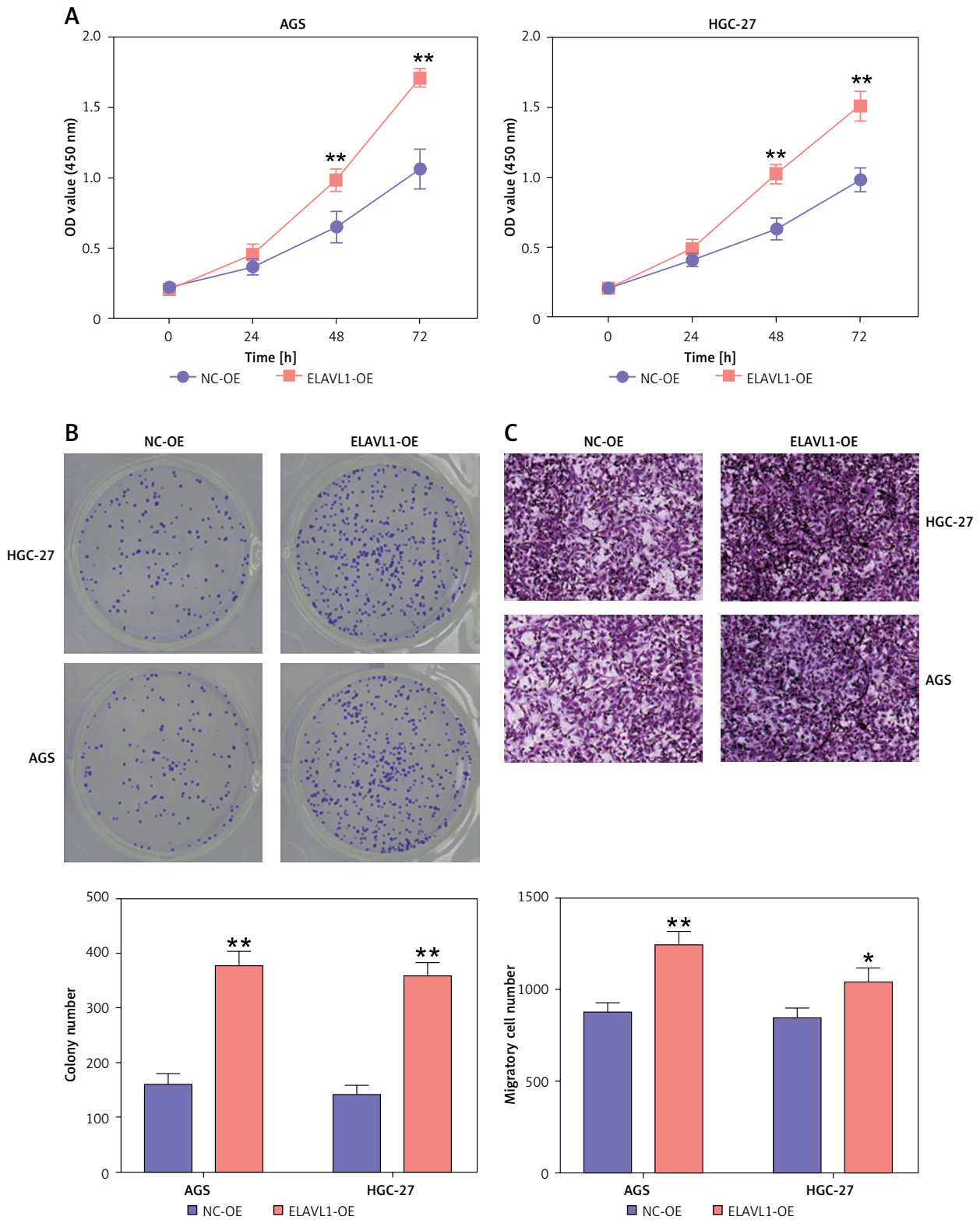


Figure 5. ELAVL1 overexpression enhances GA malignancy *in vitro*. **A** – Cell viability of HGC-27 and AGS cells transfected with ELAVL1 overexpression (ELAVL1-OE) or negative control (NC-OE) was assessed via CCK-8 assay. **B** – Cell proliferation of HGC-27 and AGS cells transfected with ELAVL1-OE or NC-OE was revealed via colony formation assay. **C** – Cell migration of HGC-27 and AGS cells transfected with ELAVL1-OE or NC-OE was revealed via Transwell assay. * $P < 0.05$, ** $p < 0.001$ vs. NC-OE

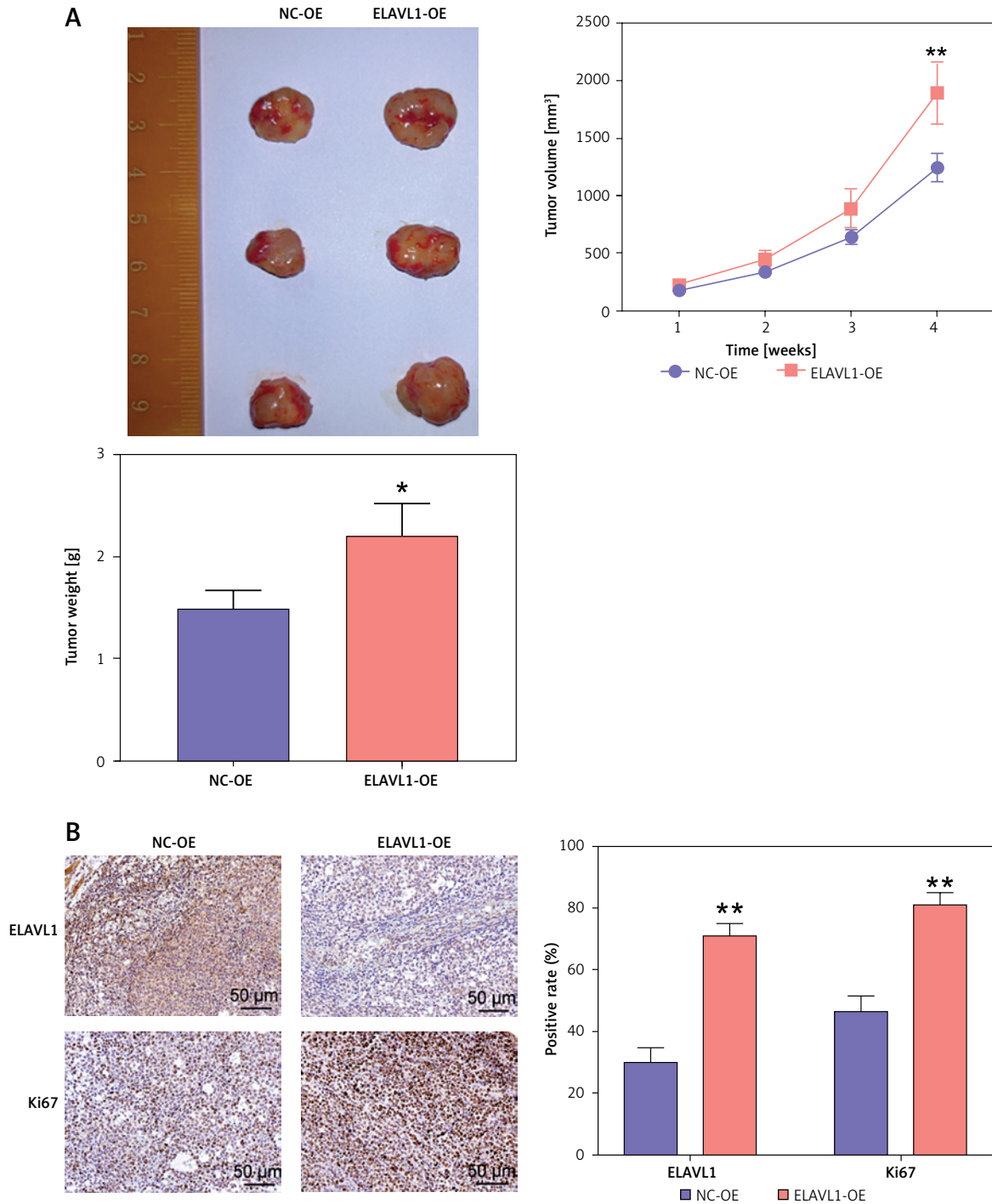


Figure 6. ELAVL1 overexpression promotes tumor growth *in vivo*. **A** – The effect of ELAVL1 overexpression on tumor growth was detected via an *in vivo* experiment. **B** – The effect of ELAVL1 overexpression on expression of Ki67 and ELAVL1 was assessed via IHC assay. * $P < 0.05$, ** $p < 0.001$ vs. NC-OE

hibition of GA cell malignancy is observed upon knocking down hsa_circ_0035277. In addition, the present study also innovatively proved that ELAVL1 could regulate m⁶A modification of hsa_circ_0035277 by binding to hsa_circ_0035277 in GA, thereby stabilizing hsa_circ_0035277 levels. Our findings establish a theoretical foundation for diagnosing GA based on exosomal hsa_circ_0035277.

Funding

No external funding.

Ethical approval

Approval number: WHZY2022-C48-01.

Conflict of interest

The authors declare no conflict of interest.

References

- Sung H, Ferlay J, Siegel RL, et al. Global Cancer Statistics 2020: GLOBOCAN estimates of incidence and mortality worldwide for 36 cancers in 185 countries. *CA Cancer J Clin* 2021; 71: 209-49.
- Necula L, Matei L, Dragu D, et al. Recent advances in gastric cancer early diagnosis. *World J Gastroenterol* 2019; 25: 2029-44.
- Patel TH, Cecchini M. Targeted therapies in advanced gastric cancer. *Curr Treat Options Oncol* 2020; 21: 70.
- Sexton RE, Hallak MNA, Uddin MH, Diab M, Azmi AS. Gastric cancer heterogeneity and clinical outcomes. *Technol Cancer Res Treat* 2020; 19: 1533033820935477.
- Wee S, Dhanak D, Li H, et al. Targeting epigenetic regulators for cancer therapy. *Ann N Y Acad Sci* 2014; 1309: 30-6.
- Vo JN, Cieslik M, Zhang Y, et al. The landscape of circular RNA in cancer. *Cell* 2019; 176: 869-81.
- Li J, Sun D, Pu W, Wang J, Peng Y. Circular RNAs in cancer: biogenesis, function, and clinical significance. *Trends Cancer* 2020; 6: 319-36.
- Wu S, Lu J, Zhu H, et al. A novel axis of circKIF4A-miR-637-STAT3 promotes brain metastasis in triple-negative breast cancer. *Cancer Lett* 2024; 581: 216508.
- Du W, Yin F, Zhong Y, et al. CircUCP2 promotes the tumor progression of non-small cell lung cancer through the miR-149/UCP2 pathway. *Oncol Res* 2023; 31: 929-36.
- Liu A, Jiang B, Song C, et al. Isoliquiritigenin inhibits circ0030018 to suppress glioma tumorigenesis via the miR-1236/HER2 signaling pathway. *MedComm (2020)* 2023; 4: e282.
- Yang F, Ma Q, Huang B, et al. CircNFATC3 promotes the proliferation of gastric cancer through binding to IGF2BP3 and restricting its ubiquitination to enhance CCND1 mRNA stability. *J Transl Med* 2023; 21: 402.
- Li WD, Wang HT, Huang YM, et al. Circ_0003356 suppresses gastric cancer growth through targeting the miR-668-3p/SOCS3 axis. *World J Gastrointest Oncol* 2023; 15: 787-809.
- Li T, Shao Y, Fu L, et al. Plasma circular RNA profiling of patients with gastric cancer and their droplet digital RT-PCR detection. *J Mol Med (Berl)* 2018; 96: 85-96.
- Kalluri R, LeBleu VS. The biology, function, and biomedical applications of exosomes. *Science* 2020; 367: eaau6977.
- Zhang H, Lu J, Liu J, Zhang G, Lu A. Advances in the discovery of exosome inhibitors in cancer. *J Enzyme Inhib Med Chem* 2020; 35: 1322-30.
- Zhang X, Wang S, Wang H, et al. Circular RNA circNRIP1 acts as a microRNA-149-5p sponge to promote gastric cancer progression via the AKT1/mTOR pathway. *Mol Cancer* 2019; 18: 20.
- Yang G, Tan J, Guo J, Wu Z, Zhan Q. Exosome-mediated transfer of circ_0063526 enhances cisplatin resistance in gastric cancer cells via regulating miR-449a/SHMT2 axis. *Anticancer Drugs* 2022; 33: 1047-57.
- Frye M, Harada BT, Behm M, He C. RNA modifications modulate gene expression during development. *Science* 2018; 361: 1346-9.
- Kumari R, Ranjan P, Suleiman ZG, et al. mRNA modifications in cardiovascular biology and disease: with a focus on m6A modification. *Cardiovasc Res* 2022; 118: 1680-92.
- Roundtree IA, Evans ME, Pan T, He C. Dynamic RNA modifications in gene expression regulation. *Cell* 2017; 169: 1187-200.
- Zhang X, Lu N, Wang L, et al. Recent advances of m(6)A methylation modification in esophageal squamous cell carcinoma. *Cancer Cell Int* 2021; 21: 421.
- Fan HN, Chen ZY, Chen XY, et al. METTL14-mediated m(6)A modification of circORC5 suppresses gastric cancer progression by regulating miR-30c-2-3p/AKT1S1 axis. *Mol Cancer* 2022; 21: 51.
- Zhang C, Wang J, Geng X, et al. Circular RNA expression profile and m6A modification analysis in poorly differentiated adenocarcinoma of the stomach. *Epigenomics* 2020; 12: 1027-40.
- Wang M, Yu F, Li P, Wang K. Emerging function and clinical significance of exosomal circRNAs in cancer. *Mol Ther Nucleic Acids* 2020; 21: 367-83.
- Mathieu M, Martin-Jaular L, Lavie G, Thery C. Specificities of secretion and uptake of exosomes and other extracellular vesicles for cell-to-cell communication. *Nat Cell Biol* 2019; 21: 9-17.
- Li D, Li L, Cao Y, Chen X. Downregulation of LINC01140 is associated with adverse features of breast cancer. *Oncol Lett* 2020; 19: 1157-64.
- Jia Y, Chen Y, Wang Q, et al. Exosome: emerging biomarker in breast cancer. *Oncotarget* 2017; 8: 41717-33.
- Yang C, Wu S, Mou Z, et al. Exosome-derived circTRPS1 promotes malignant phenotype and CD8+ T cell exhaustion in bladder cancer microenvironments. *Mol Ther* 2022; 30: 1054-70.
- Zheng R, Zhang K, Tan S, et al. Exosomal circLPAR1 functions in colorectal cancer diagnosis and tumorigenesis through suppressing BRD4 via METTL3-eIF3h interaction. *Mol Cancer* 2022; 21: 49.
- Xie M, Yu T, Jing X, et al. Exosomal circSHKBP1 promotes gastric cancer progression via regulating the miR-582-3p/HUR/VEGF axis and suppressing HSP90 degradation. *Mol Cancer* 2020; 19: 112.
- Cai Z, Xu H, Bai G, et al. ELAVL1 promotes prostate cancer progression by interacting with other m6A regulators. *Front Oncol* 2022; 12: 939784.
- Li K, Huang F, Li Y, et al. Stabilization of oncogenic transcripts by the IGF2BP3/ELAVL1 complex promotes tumorigenicity in colorectal cancer. *Am J Cancer Res* 2020; 10: 2480-94.
- Yue B, Song C, Yang L, et al. METTL3-mediated N6-methyladenosine modification is critical for epithelial-mesenchymal transition and metastasis of gastric cancer. *Mol Cancer* 2019; 18: 142.
- Cao S, Li C, Li L, Zhou G, Jiang Y, Feng J. Circular RNA hsa_circ_0000848 regulates cardiomyocyte proliferation and apoptosis under hypoxia via recruiting ELAVL1 and stabilizing SMAD7 mRNA. *Anatol J Cardiol* 2022; 26: 189-97.
- Liu H, Lan T, Li H, et al. Circular RNA circDLC1 inhibits MMP1-mediated liver cancer progression via interaction with HuR. *Theranostics* 2021; 11: 1396-411.
- Chen Y, Yang F, Fang E, et al. Circular RNA circAGO2 drives cancer progression through facilitating HuR-repressed functions of AGO2-miRNA complexes. *Cell Death Differ* 2019; 26: 1346-64.
- Li P, Xiao W. Circ_0005758 impedes gastric cancer progression through miR-1229-3p/GCNT4 feedback loop. *Toxicol In Vitro* 2022; 85: 105454.
- Yang C, Deng S. Hsa_circ_0017728 as an oncogene in gastric cancer by sponging miR-149 and modulating the IL-6/STAT3 pathway. *Arch Med Sci* 2022; 18: 1558-71.
- Shen D, Zhao H, Zeng P, et al. Circular RNA hsa_circ_0005556 accelerates gastric cancer progression by sponging miR-4270 to increase MMP19 expression. *J Gastric Cancer* 2020; 20: 300-12.